Geoscience Letters

RESEARCH LETTER

Open Access

Externally forced symmetric warming in the Arctic and Antarctic during the second half of the twentieth century

Jianyu Liu[1,2,3], Yiyong Luo[1,2,3*] and Fukai Liu[1,2,3*]

Abstract

In recent decades, the two polar regions have exhibited strikingly different changes, with much greater warming in the Arctic than the Antarctic. However, the warming asymmetry between the two polar regions is quite small during the second half of the twentieth century. By using a multi-member ensemble of simulations with the Community Earth System Model, this study investigates the relative contributions of greenhouse gases, aerosol, and ozone forcings to the responses of Arctic and Antarctic surface temperature during 1955–2000. Results show that both the greenhouse gases- and aerosols-induced changes are greater in the Arctic than in the Antarctic, yet they are opposite and act to balance each other, leaving a limited warming in the Arctic and hence a small bipolar asymmetry. Using a radiative kernel, feedback analysis reveals that both greenhouse gases and aerosol forcings influence the polar surface temperature through albedo feedback related to sea ice changes and lapse rate feedback related to strong surface temperature inversion. The ozone forcing can hardly excite any surface temperature changes over the polar regions even in the Antarctic with the strongest ozone depletion, which is due to a cancellation between the cooling effect from radiative forcing and cloud radiative feedback, and the warming effect from lapse rate feedback and enhanced atmospheric heat transport from lower latitudes.

Keywords: Arctic, Antarctic, Surface temperature, Ozone depletion, Lapse rate feedback, Atmospheric heat transport

Introduction

During the past two decades, a robust feature in both observed and modeled surface temperature changes is the enhanced warming over the Arctic, known as the famous Arctic amplification (Holland and Bitz 2003; Serreze and Francis 2006; Serreze and Barry 2011; Cohen et al. 2014; Stuecker et al. 2018). By contrast, the warming in the Antarctic is relatively modest and is largely spatially heterogeneous (Doran et al. 2002; Li et al. 2021). In particular, the Antarctic Peninsula is found to be a region with one of the largest warming trends since the 1950s, whereas the Southern Ocean and the eastern Antarctic have experienced little warming, and even cooling, over recent decades (Thompson et al. 2011; Armour et al. 2016; Oliva et al. 2017). This asymmetric surface temperature change between the two polar regions has global climatic, ecological, and social impacts, and thus its underlying mechanisms have been investigated as a hotspot (Turner et al. 2005; Masson-Delmotte et al. 2006; Hall 2010).

However, the bipolar asymmetry only becomes significant in the recent decades (Fig. 1a). During the second half of the twentieth century, the observed surface temperature changes in the two polar regions are in nearly equal magnitude, exhibiting a symmetric warming feature. It is unclear whether the absence of the bipolar warming asymmetry during this period was rooted in externally forced response or internally generated

*Correspondence: yiyongluo@ouc.edu.cn; fliu@ouc.edu.cn
[1] Frontier Science Center for Deep Ocean Multispheres and Earth System (FDOMES) and Physical Oceanography Laboratory, Ocean University of China, Qingdao, China
Full list of author information is available at the end of the article

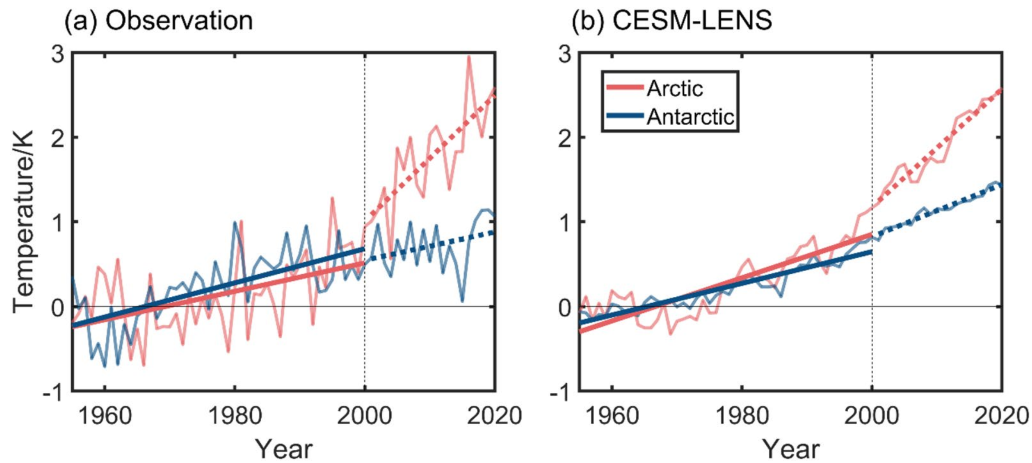

Fig. 1 Time series of surface temperature change (*K*) over the Arctic (red) and the Antarctic (blue) in **a** Berkeley Earth's primary product and **b** CESM-LENS. The temperature change is relative to a monthly climatological mean obtained by averaging over 1951–1980. The thick solid and dashed lines represent linear trends from 1955 to 2000 and from 2000 to 2020, respectively

variability. A recent paper by England (2021) pointed out that the detrended surface temperature variabilities in the Arctic and the Antarctic since the 1920s are determined by external forcings and Pacific decadal variability, respectively. However, they mainly analyzed the multi-decadal oscillation around a linear trend since the 1920s, while in this paper we focus on the bipolar symmetric warming trend during 1955–2000 and the related maintaining mechanisms.

For the surface temperature changes in the Arctic, many previous observational and modeling studies ascribed an important role to the effects of increasing greenhouse gases (GHG) and the related radiative feedbacks (Holland and Bitz 2003; Stroeve et al. 2012; Zhang et al. 2018; Liu et al. 2018, 2020). Overall, the GHG forcing can contribute about 2.43 W m^{-2} to the direct radiative forcing of global temperature change (Houghton et al. 2001). In addition, the GHG-induced warming is further amplified by albedo feedback related to sea ice melting and lapse rate feedback associated with the vertical structure of the atmospheric warming (Budyko 1969; Alexeev et al. 2005; Cai 2005; Screen and Simmonds 2010; Pithan and Mauritsen 2014; Burt et al. 2016; Goosse et al. 2018; Stuecker et al. 2018). However, GHG concentration has shown a rapid increase since the 1950s (Additional file 1: Fig. S1), then why did the accelerated Arctic warming occur in recent decades? It is reasonable to speculate that other anthropogenic forcings and/or natural variability might contribute. For instance, increased anthropogenic aerosol (AER) forcing is found to have mediated the GHG-induced warming in the Arctic (Emori et al. 1999; Myhre et al. 2014; Bellouin et al. 2020; Cohen et al. 2020; England et al. 2021). In addition, some AER, like black carbon, can effectively reduce the surface albedo through deposition on snow and ice and hence play a warming effect in the Arctic (Flanner et al. 2007; He et al. 2014; Qian et al. 2015). As for the ozone forcing, although the ozone depletion (OD) is confined to the Southern Hemisphere, increased Ozone-depleting substances are observed in the Northern Hemisphere, which traps more outgoing longwave radiation and thus contributes positively to the Arctic warming (Ramanathan et al. 1987; Shine 1991; Marshall et al. 2014; Virgin and Smith 2019; Polvani et al. 2020).

For the Antarctic, on the one hand, the warming pattern is likely modulated by atmospheric circulation associated with internally generated variability (Vaughan et al. 2003; Mayewski et al. 2009; Steig et al. 2009; England, 2021; Tewari et al. 2021). For example, the rapid warming over West Antarctic in recent decades is found to be related to the multi-decadal sea surface temperature variability in the North Atlantic and tropical Pacific (Ding et al. 2011; Wang et al. 2020; Eayrs et al. 2021). On the other hand, the surface temperature changes in the Antarctic are also affected by external forcings, especially the anthropogenic emissions of ozone-depleting substances. For example, the OD in the Antarctic lower stratosphere is found to be responsible for the poleward shift of the Southern Hemisphere atmospheric circulation during the austral summer over the second half of the twentieth century (Thompson et al. 2000; Polvani et al. 2011; Fogt and Marshall 2020), which further contributes to the rapid warming over the Antarctic Peninsula through advecting warm air from lower latitudes and enhancing ocean upwelling that transports warmer water from the subsurface to the surface (Solomon et al.

1986; Turner et al. 2005; Monaghan et al. 2008; Joughin et al. 2012; Pritchard et al. 2012; Li et al. 2014; Wang et al. 2020). However, by analyzing climate model outputs, Polvani et al. (2021) found that the Southern Annular Mode change due to the OD has limited influence on the sea ice expansion around Antarctica in recent decades.

Since the externally excited climate response is tangled with the internally generated low-frequency variability, it is extremely challenging to identify the relative roles of different external forcings in shaping the climate change in the polar regions, not to mention their contributions to the symmetric responses between the Arctic and the Antarctic during the second half of the twentieth century. One possible approach to help us better understand the problem is to employ large ensembles of the same model initialized with the different conditions but perturbed by the same external forcing. With ensemble member mean, we can separate the externally forced response from the internally generated variability to a large extent.

By employing the Community Earth System Model large ensemble (Kay et al. 2015), this study performs an analysis on the relative roles of three major climate drivers (i.e., GHG, AER, and OD) on the radiative forcing and related feedbacks over the polar climate, as well as the bipolar symmetric warming during the second half of the twentieth century. As is shown later, we find that the OD forcing, although being strong over the Antarctic, can hardly excite any surface temperature changes over the polar regions due to the cancellation between the changes in lapse rate feedback, the cloud feedback, and the atmospheric heat transport. The GHG forcing indeed favors the generation of Arctic amplification with greater warming in the Arctic than the Antarctic, however, the AER forcing induces a greater cooling in the Arctic and substantially mitigates the bipolar asymmetry. "Data and methods" section leads on to "Results" section that presents the polar surface temperature changes induced by individual forcing as well as the underlying mechanisms, followed by "Summary and discussion".

Data and methods

CESM-LENS

We examine the large ensemble set of historical simulations of the National Center for Atmospheric Research's Community Earth System Model version 1 (CESM-LENS; Kay et al. 2015). CESM-LENS consists of coupled atmosphere, land, ocean and sea ice models. The atmospheric component is the Community Atmosphere Model version 5 (CAM5; Kay et al. 2015) with 30 vertical levels and $1.25^{o} \times 0.94^{\circ}$ horizontal resolution. The land component, Community Land Model version 4 (CLM4; Lawrence et al. 2012), has the same horizontal resolution as CAM5. The ocean component, the Parallel Ocean Program version 2 (POP2; Danabasoglu et al. 2012), has a nominal 1° horizontal resolution with meridional grid spacing decreasing to 0.3° near the equator. Vertically, it has 60 unevenly spaced vertical layers with the highest resolution of 10 m near the surface. The sea ice component, the Community Ice CodE (CICE; Hunke et al. 2010), has the same horizontal grid as POP2.

We analyze five simulation ensembles in CESM-LENS. To enable the comparison with observations, we first use the historical ensemble consisting of 42 realizations spanning from 1920 to 2020. The three "fixed" ensembles follow the same simulation protocol as the historical ensemble, except that one forcing agent (GHG, AER, or OD) is fixed at a constant level (1920 levels for GHG and AER, 1955 level for OD; England et al. 2016; Lenaerts et al. 2018; Deser et al. 2020). Note that the GHG and AER ensembles consist of 20 members, and the OD ensemble includes 8 members. In the following analysis, we select the same number of the historical ensemble as the single forcing ensemble for the sake of equality. The Arctic and Antarctic regions are defined as 60° N–90° N and 60° S–90° S, respectively.

For any variable of interest, we first subtract individual forcing-fixed ensemble from the historical ensemble and average over 1955–2000. Then, the response to the individual forcing is obtained with the average further subtracting a base value, which is defined as a mean over 1945–1965 for the GHG- and AER-fixed ensembles, and 1955 for the OD-fixed ensemble (since this set of experiments start from 1955). Note that the base value has been tested with different time periods and the results are essentially the same.

Radiative kernels

The energy balance of an atmospheric column in an equilibrium state is among the top-of-atmosphere (TOA) heat flux (F'_{TOA}), the surface heat flux (F'_{s}), and the convergence of the vertically integrated atmospheric heat transport ($\nabla \cdot F'$):

$$0 = F'_{\mathrm{TOA}} + F'_{\mathrm{s}} + \nabla \cdot F', \quad (1)$$

where prime indicates the difference between two simulations. Changes in atmospheric energy storage are very small and set to zero in this equation. To evaluate the contributions from various physical processes, we employ the radiative kernel method (Soden et al. 2008) to decompose the TOA radiative anomalies (F'_{TOA}) into contributions from different radiative feedbacks:

$$F'_{\mathrm{TOA}} = R_{\mathrm{F}} + R'_{\mathrm{PLK}} + R'_{\mathrm{LPS}} + R'_{\mathrm{ALB}} + R'_{\mathrm{WV}} + R'_{\mathrm{CLD}}, \quad (2)$$

where R_{F} represents the instantaneous radiative forcings, with the GHG forcing being obtained from GISS modelE

(Hansen et al. 2007), and the AER and OD forcings from ACCMIP (Lamarque et al. 2013), respectively. The rest of the terms in Eq. (2) are the Planck feedback (R'_{PLK}), lapse rate feedback (R'_{LPS}), albedo feedback (R'_{ALB}), water vapor feedback (R'_{WV}), and cloud feedback (R'_{CLD}). Following Liu et al. (2018), the cloud radiative feedback is estimated as a residual of the other terms in Eq. (2) to close the energy budget. These feedbacks are adopted from the radiative kernels derived from the Rapid Radiative Transfer Model (RRTM) proposed by Huang et al. (2017).

Results

Surface temperature

Comparing Fig. 1b to a, the ensemble mean of the historical simulations in CESM-LENS can faithfully capture the observed warming trends during 1955–2000 in both polar regions, indicating that the symmetric warming feature is largely determined by external forcings rather than internal variabilities. Thus, we first examine the surface temperature changes in the historical simulations and the contributions from each individual forcing during the second half of the twentieth century (Fig. 2).

The area-weighted surface temperature response in the Arctic reaches ~0.27 K (Fig. 2a), which is more than twice of the global mean surface temperature warming (~0.10 K). While the amplified warming in the Arctic is entirely attributed to the GHG forcing (~0.73 K; Fig. 2c), AER acts to reduce it to a large extent (~−0.56 K; Fig. 2e). In contrast, the OD forcing has a very limited impact on the Arctic surface temperature (~−0.06 K; Fig. 2g).

Similar to the situation in the Arctic, the surface temperature change in the Antarctic is also characterized by an enhanced warming (~0.28 K; Fig. 2b), and the warming appears to be larger in the Indian sector of the Southern Ocean. In terms of the GHG-induced surface temperature response, the warming in the Antarctic (~0.40 K; Fig. 2d) is only about half of that in the Arctic, clearly exhibiting an Arctic amplification feature. However, different from the strong cancellation between GHG- and AER-induced responses in the Arctic, the AER-induced cooling in the Antarctic (~−0.15 K; Fig. 2f) is very weak and cannot offset the GHG-induced warming. In addition, it is somewhat striking to see the small contribution from OD (~0.03 K; Fig. 2h), since previous studies have argued that the OD forcing can exert strong influence on the Southern Hemisphere troposphere and surface temperature changes since 1950s (Solomon 1990; Randel and Wu 1999; Cionni et al. 2011; Thompson et al. 2011; Previdi and Polvani 2017; Xia et al. 2020). We will show evidence later that this small surface temperature change induced by OD is due to a cancellation between the cooling effect from radiative forcing as well as cloud radiative feedback and the warming effect from lapse rate feedback as well as atmospheric heat transport.

Radiative forcings

The area-mean radiative forcings (R_F) over the two polar regions due to GHG, AER and OD are presented in Fig. 3. Because of its well-mixed nature, the GHG-induced R_F is positive and similar in magnitude between the Arctic (~0.82 W m^{-2}) and Antarctic (~0.71 W m^{-2}). The R_F due to AER forcing is much smaller in magnitude than that to GHG forcing, and it is much larger in the Arctic (~−0.22 W m^{-2}) than in the Antarctic (~−0.09 W m^{-2}). The OD-induced R_F also appears to be asymmetric over the two polar regions, and it is quite negative in the Antarctic (~−0.38 W m^{-2}) because of the reduced downwelling longwave radiation there (Ramanathan and Dickinson 1979; Ramaswamy et al. 1992; de F. Forster and Shine 1997; Chen et al. 2007; Shindell et al. 2013; Chiodo et al. 2017; Virgin and Smith 2019).

Kernels decomposition

To understand how GHG and AER radiative forcings contribute to the symmetric surface temperature changes during the second half of the twentieth century in both polar regions, and why the OD forcing is less effective in causing the surface temperature change in the Antarctic, we decompose the TOA heat flux into radiative feedbacks based on Eq. 2.

As shown in Fig. 3, in both polar regions, the warming response to GHG forcing is mainly contributed by radiative forcing, lapse rate and albedo feedbacks. The water vapor feedback also makes a contribution, but it is quite feeble because of the dry atmosphere there (Payne et al. 2015; Held and Soden 2000). The Planck feedback is necessarily the opposite to the temperature change and is the major damping term to the warming response. The cloud radiative feedback and surface heat fluxes also act to suppress the Arctic warming but to a small magnitude. The contributions from these processes due to AER are overall opposite to those due to GHG. The above results are consistent with previous studies (Soden and Held 2006; Shell et al. 2008; Soden et al. 2008; Pithan and Mauritsen 2014; Stuecker et al. 2018).

Regarding the situation in OD, its impact occurs mainly in the Antarctic. In particular, the convergence of the vertically integrated atmospheric heat transport $(\nabla \cdot F')$ appears to be a major contributor and works to transport more energy into the Antarctic, which is quite different from its feebleness in both GHG and AER. In addition, the lapse rate feedback is another major warming process in the Antarctic. However, the warming induced by atmospheric heat transport and lapse rate feedback is largely balanced by the cooling due to cloud radiative

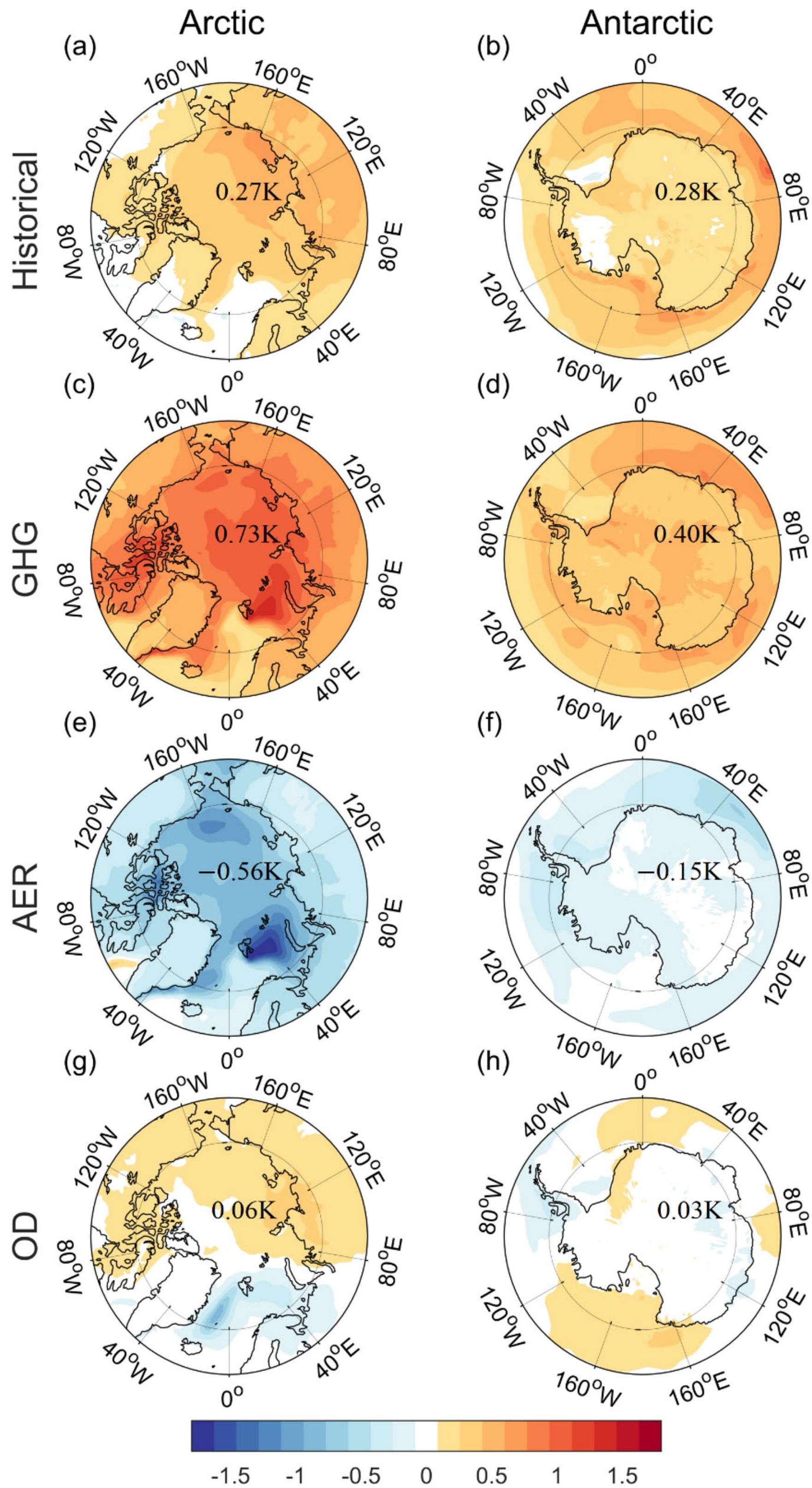

Fig. 2 Surface temperature changes (*K*) in the **a**, **b** historical simulation and the contributions from **c**, **d** GHG, **e**, **f** AER, and **g**, **h** OD over the two polar regions during 1955–2000 relative to 1945–1965 for GHG and AER and 1955 for OD. The area-weighted surface temperature anomalies are labeled in the corresponding panels

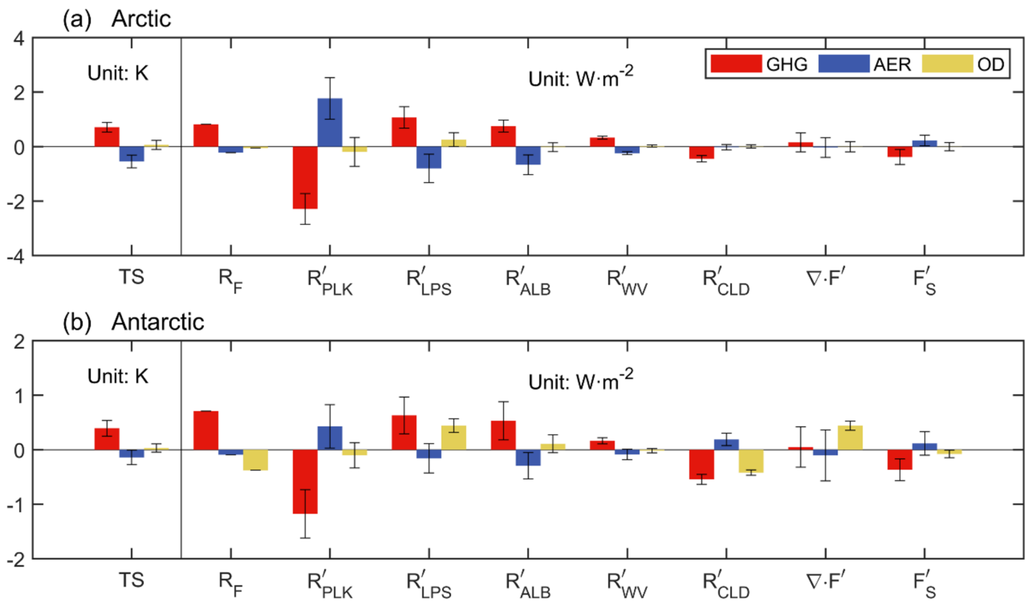

Fig. 3 Surface temperature changes (*K*) and contributions to the TOA heat flux (W m^{-2}) from radiative forcing (R_F), feedbacks of Planck (R'_{PLK}), lapse rate ((R'_{LPS}), albedo (R'_{ALB}), water vapor (R'_{WV}) and cloud (R'_{CLD}) as well as atmospheric heat convergence ($\nabla \cdot F'$) and surface heat flux (F'_S) in GHG (red bars), AER (blue bars), and OD (yellow bars) over the **a** Arctic (60°–90° S) and **b** Antarctic (60°–90° N). The error bars denote the standard deviations of values in CESM-LENS members. Note the y-axis scales in **a** and **b** are different

feedback and exerted radiative forcing, resulting in a small surface temperature change in the Antarctic.

The albedo feedback is largely proportional to sea ice cover changes and the related mechanism is quite straightforward, and thus not the focus in the following analysis. Apart from the albedo feedback, the lapse rate and cloud feedbacks, as well as atmospheric heat convergence, make significant contributions to the energy balance, especially in the Antarctic. We next examine physical mechanisms related to these processes, with a focus on the compensation relationship among them in OD.

Lapse rate feedback

The lapse rate feedback is closely related to the uneven change of vertical temperature profile (Manabe and Wetherald 1975; Wetherald and Manabe 1988). The coupling mechanisms between the surface and the upper atmosphere are quite different between the high-latitude and tropical regions, i.e., the coupling is through radiation in the former while it is through deep convection in the latter. Therefore, the lapse rate feedback is usually positive in the high latitudes and negative in the tropics (Hansen et al. 1984; Graversen et al. 2014; Pithan and Mauritsen 2014). Specifically, the GHG-forced inversion layer in the polar regions results in a larger warming in the near-surface air than in the upper troposphere (Fig. 4d, f), which leads to the return of longwave radiation and further amplifies the surface warming (Fig. 4a). Meanwhile, the deep convection in the tropics results in warmer upper troposphere than the surface (Fig. 4e), and thus the lapse rate feedback is negative there. The pattern of lapse rate feedback in AER is almost a mirror image of that in GHG in the troposphere (Fig. 4b).

However, the lapse rate feedback due to the OD forcing is positive in both high-latitude and tropical regions (Fig. 4c), a result quite different from those due to the GHG and AER forcings. Shown in Fig. 4d–f are the vertical temperature change profiles in the atmosphere under the three forcings, respectively. Deviation from the vertical uniform temperature profile will result in lapse rate feedback. It is clear that the strongest warming due to GHG and cooling due to AER occur at the lower (upper) troposphere in the polar regions (tropics), leading to positive (negative) lapse rate feedback there (Fig. 4a, b). In contrast, the strongest temperature changes due to OD occur at the bottom of the stratosphere as well as the upper troposphere, especially in the Antarctic and equatorial regions with strong OD forcing, which reduces the outward emission of longwave radiation and leads to positive lapse rate feedback there. Therefore, the lapse rate feedback due to OD is mainly determined by the atmospheric temperature structure of the stratospheric cooling, which is different from that due to GHG and AER that is controlled by the surface–troposphere coupling.

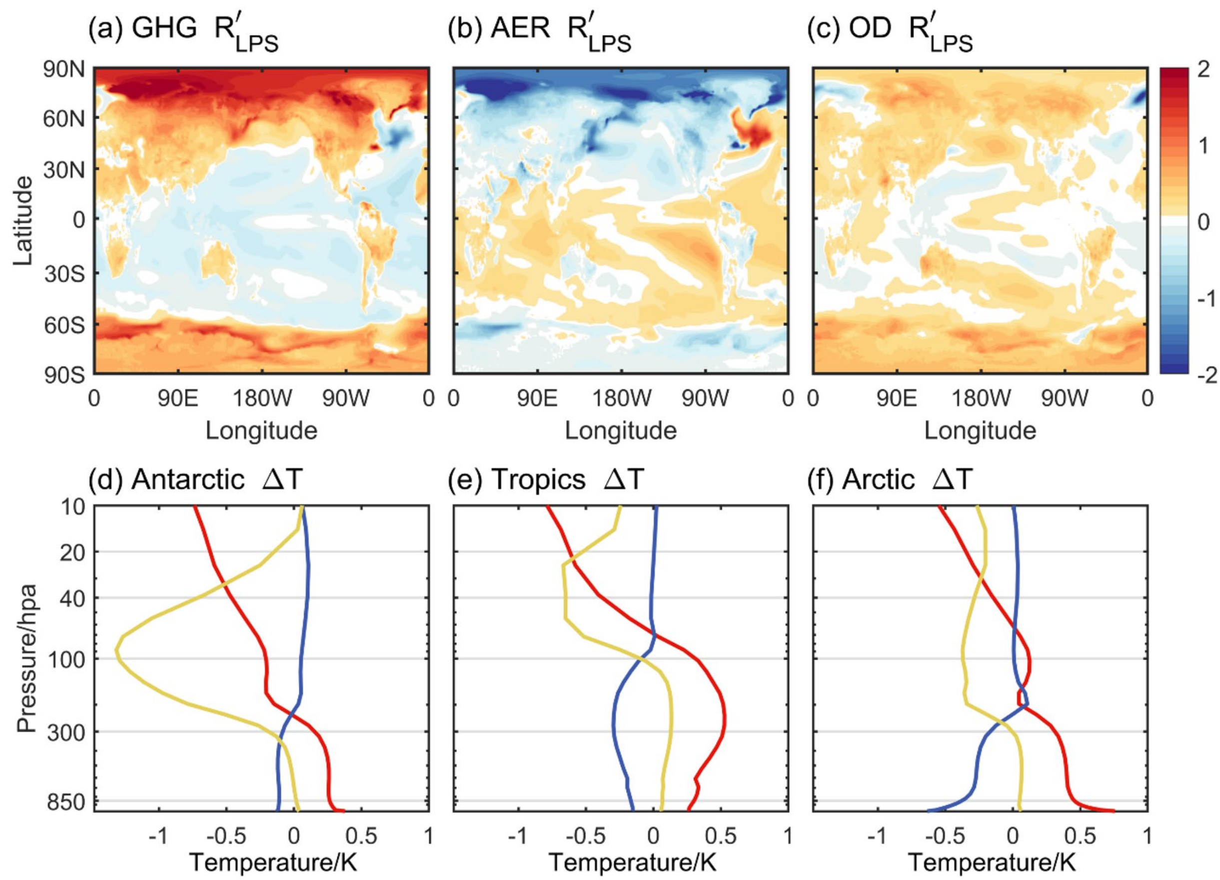

Fig. 4 Spatial pattern of lapse rate feedback contribution to the TOA heat flux (W m^{-2}) due to **a** GHG, **b** AER and **c** OD. Vertical temperature changes (*K*) in the atmosphere due to GHG (red), AER (blue), and OD (yellow) in the **d** Antarctic (60°–90° S), **e** Tropics (25° S–25° N), and **f** Arctic (60°–90° N)

Cloud radiative feedback

Over the Antarctic, the contribution from cloud radiative feedback is quite strong, especially in response to the GHG and OD forcings. We next examine the vertical temperature and cloud fraction changes in the atmosphere (Fig. 5). Both the GHG- and OD-induced atmospheric temperature changes are featured with cooling in the lower stratosphere and warming (or weak cooling) in the upper troposphere, which increases instability and local relative humidity and thus enhances the formation of high-level clouds there (Fig. 5d, f; Hansen et al. 1997; Hodnebrog et al. 2014; Xia et al. 2018). Increasing clouds reflect more solar insolation back to space in summer and thus have negative feedback on the surface temperature change. On the other hand, the increasing clouds emit more longwave radiation to the surface and thus has a warming effect (Zelinka et al. 2012). Overall, the shortwave cooling effect dominates, causing a negative cloud radiative feedback in GHG and OD over the Antarctic (Fig. 3b).

Atmospheric heat convergence

For the Arctic region, the contribution from atmospheric energy transport ($\nabla \cdot F'$ in Fig. 3a) is negligible compared to those from other major feedbacks in all three forcing scenarios, indicating that the Arctic surface temperature change is dominated by local feedbacks. For the Antarctic region, in contrast, the atmospheric heat convergence ($\nabla \cdot F'$ in Fig. 3b) induced by OD plays a critical role and acts to mediate the negative instantaneous radiative forcing.

To examine the relationship between changes in atmospheric energy transport and local energy balance over the Antarctic due to OD, we regress the anomalous TOA net heat flux $\left(F'_{\mathrm{TOA}}\right)$ against the anomalous atmospheric heat convergence ($\nabla \cdot F'$ in Fig. 6a) from 1955 to 2000. It is found that they are significantly negatively correlated with a correlation coefficient being −0.81 at the 99% confidence level, suggesting that the atmosphere works to transport more energy from lower

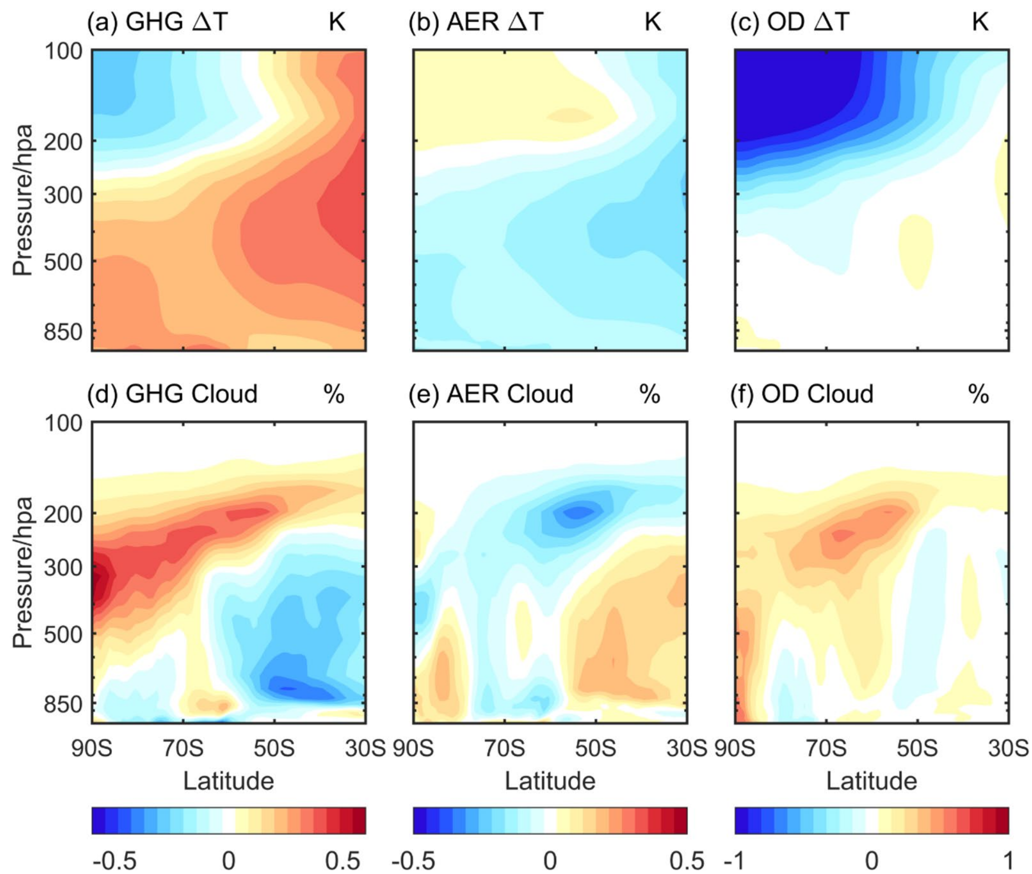

Fig. 5 Changes of zonal mean temperature (*K*) and cloud fraction (%) due to **a**, **d** GHG; **b**, **e** AER; and **c**, **f** OD forcings in the Southern Hemisphere

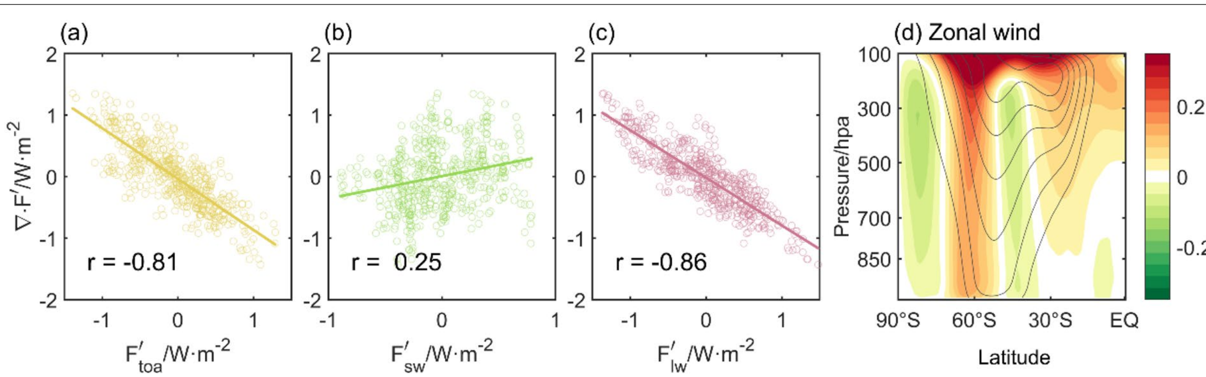

Fig. 6 Linear regression of **a** OD-induced TOA heat flux (F'_{TOA}) and its components of **b** shortwave (F'_{SW}) and (c) longwave (F'_{LW}) onto atmospheric energy convergence ($\nabla \cdot F'$) in the Antarctic (60°–90° S) during 1955–2000. Lines are a least-squares linear fit to the data, *r* is the correlation coefficient, and all of the flux variables are filtered with a 12-month running mean. **d** Zonal mean wind climatology from the historical simulation (contours) and its change due to OD (color) in the Southern Hemisphere

latitudes to the Antarctic to mediate the TOA energy imbalance exerted by the OD forcing.

A decomposition of F'_{TOA} into longwave (F'_{LW}) and shortwave (F'_{SW}) components finds that the strong negative correlation between F'_{TOA} and $\nabla \cdot F'$ is largely due to its longwave component (Fig. 6c). In particular, the OD forcing causes a strong cooling in the lower stratosphere (Fig. 5c), which in turn leads to a reduction in outward emitted longwave radiation. The reduced downwelling longwave radiation further cools the troposphere and stratosphere in the Antarctic, enlarging the meridional temperature gradient. Since the synoptic wave fluxes of heat are essentially diffusive, the increased meridional near-surface temperature gradient triggers a more complex dynamical effect (Held 1999; Grise et al. 2009). This effect on the fluxes of heat in the lower troposphere further causes a heat flux convergence in the Antarctic (Haynes et al. 1991; Song and Robinson 2004; Thompson et al. 2006). In addition, this poleward wave fluxes of heat can drive a poleward shift and a strengthening of the subpolar jet (Fig. 6d), in agreement with previous studies (Karoly 1990; Lorenz and Hartmann 2001; Thompson et al. 2011; Grise et al. 2013; Previdi and Polvani 2014; Swart et al. 2015).

In contrast, the shortwave component has limited contribution (Fig. 6b) because the high albedo over the Antarctic region reflects most of the downward shortwave back to space. This is further supported by the close-to-zero albedo feedback in the Antarctic (Fig. 3b), indicating that the OD forcing has only a small impact on sea ice changes (not shown).

Summary and discussion

During the second half of the twentieth century when anthropogenic forcings were strong, both the observations and model simulations show a symmetric warming between the Arctic and the Antarctic, which is in sharp contrast to the Arctic amplification and strong bipolar asymmetric warming during the recent decades. While the latter has been extensively studied, this study examines the symmetric warming in the Arctic and Antarctic during 1955–2000 and identify the relative contributions from GHG, AER, and OD by employing the CESM-LENS. We find that the OD forcing has little impact even in the Antarctic where the ozone depletion is the strongest, and the GHG-induced warming in the Arctic is largely mitigated by the AER-induced cooling. Taken together, there appears to be a small warming asymmetry between the Arctic and Antarctic.

We quantitatively partition the surface temperature changes into contributions from various climate feedbacks by using radiative kernels. It is found that GHG induces surface temperature changes mainly through lapse rate feedback and albedo feedback in both polar regions, and the feedbacks are stronger in the Arctic than the Antarctic. The AER-induced cooling in both polar regions also works through the lapse rate and albedo feedbacks, and mitigates largely the warming induced by GHG.

Although the OD forcing induces strong cooling in the lower stratosphere over the Antarctic region, its impact on the local surface temperature is rather small. A further analysis finds that the lapse rate feedback and atmospheric heat transport cause significant warming in the Antarctic, which, however, is cancelled out by the cooling effect from the OD radiative forcing and cloud radiative feedback. The warming effect from the lapse rate feedback and atmospheric heat transport is related to the strong stratosphere cooling, which inhibits the outgoing longwave radiation and results in a negative lapse rate feedback. On the other hand, the decrease in the TOA heat flux due to the reduced outgoing longwave radiation is balanced by atmospheric heat transport from lower latitudes to the Antarctic, leading to a strong atmospheric heat convergence there. Moreover, the stratospheric cooling is also responsible for the strong negative cloud feedback, and causes instability in the upper troposphere and promotes the amount of high cloud, resulting in a surface cooling in the Antarctic.

The results in this study are mainly based on single model large ensembles. To validate the robustness of our results, we further analyze the large ensemble of second Generation Canadian Earth System Model (CanESM-LENS) experiments, which consists of 50 realizations spanning over 1950–2020. Overall, the results from CanESM-LENS are in good agreement with those from CESM-LENS. For example, CanESM-LENS can also capture the symmetric warming between the two polar regions during the second half of the twentieth century (Additional file 1: Fig. S2). The OD forcing can hardly excite any surface temperature changes over the Antarctic region (Additional file 1: Fig. S3). Therefore, this above agreement between the two large ensemble experiments suggests that the major conclusions of our study are not model-dependent.

It should be noted that the complex cloud feedback is estimated as a residual in this analysis, and thus errors and uncertainties associated with other feedbacks and nonlinear processes are all included in the cloud feedback. In addition, the simulations of the fixed ozone are performed with only 8 members, and thus influence from internal variability may still exist to some extent. However, the current results can successfully capture the strong cooling in the lower stratosphere and the poleward shift of the westerly jets that have been revealed by many previous studies, giving us confidence that the results discussed in this study are reliable.

Abbreviations

GHG: Greenhouse gases; AER: Aerosol; OD: Ozone depletion; CESM-LENS: Community Earth System Model version 1 Large Ensemble; CAM5: Community Atmosphere Model version 5; CLM4: Community Land Model version 4; POP2: Parallel Ocean Program version 2; CICE: Community Ice CodE; TOA: Top-of-atmosphere; RRTM: Rapid Radiative Transfer Model; AOD: Aerosol optical depth; CanESM-LENS: The Second Generation Canadian Earth System Model Large Ensemble.

Supplementary Information

The online version contains supplementary material available at https://doi.org/10.1186/s40562-022-00226-x.

Additional file 1. Supplementary.

Acknowledgements

The authors are grateful to the editor and two anonymous reviewers who provided extremely insightful and valuable feedback and suggestions. This work is supported by the National Key Research and Development Program of China (2018YFA0605702) and the National Natural Science Foundation of China (NSFC; 41976006, 91858210, and 41906002).

Author contributions

YL and FL conceived the study. JL conducted the analysis, drew the figures, and wrote the first draft of the paper. YL and FL helped interpret the results and forge the storyline of the paper. All authors provided comments on different versions of the paper. All authors read and approved the final manuscript.

Funding

This work is supported by NSFC through grants of 41976006, 91858210, and 41906002.

Availability of data and materials

The CESM-LENS datasets are accessible from https://www.earthsystemgrid.org/dataset/ucar.cgd.ccsm4.cesmLE.html. The CanESM-LENS datasets are accessible from http://crd-data-donnees-rdc.ec.gc.ca/CCCMA/products/CanSISE/output/CCCma/CanESM2/. The GHG radiative forcing dataset is accessible from https://data.giss.nasa.gov/modelE/transient/climsim.html, and the AER and OD forcings datasets are accessible from https://www.giss.nasa.gov/projects/accmip/. The surface temperature dataset is accessible from http://berkeleyearth.org/data/.

Declarations

Competing interests

The authors declare that they have no competing interests.

Author details

[1]Frontier Science Center for Deep Ocean Multispheres and Earth System (FDOMES) and Physical Oceanography Laboratory, Ocean University of China, Qingdao, China. [2]Qingdao National Laboratory for Marine Science and Technology, Qingdao, China. [3]College of Oceanic and Atmospheric Sciences, Ocean University of China, Qingdao, China.

Received: 31 December 2021 Accepted: 8 April 2022
Published online: 27 April 2022

References

Alexeev VA, Langen PL, Bates JR (2005) Polar amplification of surface warming on an aquaplanet in "ghost forcing" experiments without sea ice feedbacks. Clim Dyn 24(7–8):655–666
Armour KC, Marshall J, Scott JR, Donohoe A, Newsom ER (2016) Southern Ocean warming delayed by circumpolar upwelling and equatorward transport. Nat Geosci 9(7):549–554
Bellouin N, Quaas J, Gryspeerdt E, Kinne S, Stier P, Watson-Parris D et al (2020) Bounding global aerosol radiative forcing of climate change. Rev Geophys. https://doi.org/10.1029/2019RG000660
Budyko MI (1969) The effect of solar radiation variations on the climate of the Earth. Tellus 21(5):611–619
Burt MA, Randall DA, Branson MD (2016) Dark warming. J Clim 29:705–719
Cai M (2005) Dynamical amplification of polar warming. Geophys Res Lett. https://doi.org/10.1029/2005GL024481
Chen WT, Liao H, Seinfeld JH (2007) Future climate impacts of direct radiative forcing of anthropogenic aerosols, tropospheric ozone, and long-lived greenhouse gases. J Geophys Res Atmos. https://doi.org/10.1029/2006JD008051
Chiodo G, Polvani LM, Previdi M (2017) Large increase in incident shortwave radiation due to the ozone hole offset by high climatological albedo over Antarctica. J Clim 30(13):4883–4890
Cionni I, Eyring V, Lamarque JF, Randel WJ, Stevenson DS, Wu F, Bodeker GE, Shepherd TG, Shindell DT, Waugh DW (2011) Ozone database in support of CMIP5 simulations: results and corresponding radiative forcing. Atmos Chem Phys 11(21):11267–11292
Cohen J, Screen JA, Furtado JC, Barlow M, Whittleston D, Coumou D, Francis J, Dethloff K, Entekhabi D, Overland J, Jones J (2014) Recent Arctic amplification and extreme mid-latitude weather. Nat Geosci 7(9):627–637
Cohen J, Zhang X, Francis J, Jung T, Kwok R, Overland J, Ballinger TJ, Bhatt US, Chen HW, Coumou D, Feldstein S, Gu H, Handorf D, Henderson G, Ionita M, Kretschmer M, Laliberte F, Lee S, Linderholm HW, Maslowski W, Peings Y, Pfeiffer K, Rigor I, Semmler T, Stroeve J, Taylor PC, Vavrus S, Vihma T, Wang S, Wendisch M, Wu Y, Yoon J (2020) Divergent consensuses on Arctic amplification influence on midlatitude severe winter weather. Nat Clim Change 10(1):20–29
Danabasoglu G, Bates SC, Briegleb BP, Jayne SR, Jochum M, Large WG, Peacock S, Yeager SG (2012) The CCSM4 ocean component. J Clim 25(5):1361–1389
de F. Forster PM, Shine KP (1997) Radiative forcing and temperature trends from stratospheric ozone changes. J Geophys Res Atmos 102(D9):10841–10855.
Deser C, Phillips AS, Simpson IR, Rosenbloom N, Coleman D, Lehner F, Pendergrass AG, DiNezio P, Stevenson S (2020) Isolating the evolving contributions of anthropogenic aerosols and greenhouse gases: a new CESM1 large ensemble community resource. J Clim 33(18):7835–7858
Ding Q, Steig EJ, Battisti DS, Küttel M (2011) Winter warming in West Antarctica caused by central tropical Pacific warming. Nat Geosci 4(6):398–403
Doran PT, Priscu JC, Lyons WB, Walsh JE, Fountain AG, McKnight DM, Moorhead DL, Virginia RA, Wall DH, Clow GD, Fritsen CH, McKay CP, Parsons AN (2002) Antarctic climate cooling and terrestrial ecosystem response. Nature 415(6871):517–520
Eayrs C, Li X, Raphael MN, Holland DM (2021) Rapid decline in Antarctic sea ice in recent years hints at future change. Nat Geosci 14(7):460–464
Emori S, Nozawa T, Abe-Ouchi A, Numaguti A, Kimoto M, Nakajima T (1999) Coupled ocean-atmosphere model experiments of future climate change with an explicit representation of sulfate aerosol scattering. J Meteorol Soc Jpn Ser II 77(6):1299–1307
England MR (2021) Are multi-decadal fluctuations in Arctic and Antarctic surface temperatures a forced response to anthropogenic emissions or part of internal climate variability? Geophys Res Lett. https://doi.org/10.1029/2020GL090631
England MR, Polvani LM, Smith KL, Landrum L, Holland MM (2016) Robust response of the Amundsen Sea Low to stratospheric ozone depletion. Geophys Res Lett 43(15):8207–8213
England MR, Eisenman I, Lutsko NJ, Wagner TJ (2021) The recent emergence of Arctic amplification. Geophys Res Lett. https://doi.org/10.1029/2021GL094086
Flanner MG, Zender CS, Randerson JT, Rasch PJ (2007) Present-day climate forcing and response from black carbon in snow. J Geophys Res Atmos. https://doi.org/10.1029/2006JD008003
Fogt RL, Marshall GJ (2020) The Southern Annular Mode: variability, trends, and climate impacts across the southern Hemisphere. Wiley Interdiscip Rev Clim Change 11(4):e652
Goosse H, Kay JE, Armour KC, Bodas-Salcedo A, Chepfer H, Docquier D, Jonko A, Kushner PJ, Lecomte O, Massonnet F, Park H-S, Pithan F, Svensson G, Vancoppenolle M (2018) Quantifying climate feedbacks in polar regions. Nat Commun 9(1):1–13
Graversen RG, Langen PL, Mauritsen T (2014) Polar amplification in CCSM4: contributions from the lapse rate and surface albedo feedbacks. J Clim 27(12):4433–4450
Grise KM, Thompson DW, Forster PM (2009) On the role of radiative processes in stratosphere–troposphere coupling. J Clim 22(15):4154–4161

Grise KM, Polvani LM, Tselioudis G, Wu Y, Zelinka MD (2013) The ozone hole indirect effect: cloud-radiative anomalies accompanying the poleward shift of the eddy-driven jet in the southern Hemisphere. Geophys Res Lett 40(14):3688–3692
Hall CM (2010) Tourism and environmental change in polar regions: impacts, climate change and biological invasion. Tourism and change in polar regions. Routledge, London, pp 60–88
Hansen J, Lacis A, Rind D, Russell G, Stone P, Fung I, Ruedy R, Lerner J (1984) Climate sensitivity: analysis of feedback mechanisms. Feedback 1:1–3
Hansen J, Sato M, Ruedy R (1997) Radiative forcing and climate response. J Geophys Res Atmos 102(D6):6831–6864
Hansen J, Sato M, Ruedy R, Kharecha P, Lacis A, Miller R, Nazarenko L, Lo K, Schmidt GA, Russell G, Aleinov I, Bauer S, Baum E, Cairns B, Canuto V, Chandler M, Cheng Y, Cohen A, Del Genio A, Faluvegi G, Fleming E, Friend A, Hall T, Jackman C, Jonas J, Kelley M, Kiang NY, Koch D, Labow G, Lerner J, Menon S, Novakov T, Oinas V, Perlwitz Ja, Perlwitz Ju, Rind D, Romanou A, Schmunk R, Shindell D, Stone P, Sun S, Streets D, Tausnev N, Thresher D, Unger N, Yao M, Zhang S (2007) Climate simulations for 1880–2003 with GISS modelE. Clim Dyn 29(7):661–696
Haynes PH, McIntyre ME, Shepherd TG, Marks CJ, Shine KP (1991) On the "downward control" of extratropical diabatic circulations by eddy-induced mean zonal forces. J Atmos Sci 48(4):651–678
He C, Li Q, Liou KN, Takano Y, Gu Y, Qi L, Mao Y, Leung LR (2014) Black carbon radiative forcing over the Tibetan Plateau. Geophys Res Lett 41(22):7806–7813
Held IM (1999) The macroturbulence of the troposphere. Tellus A 51(1):59–70
Held IM, Soden BJ (2000) Water vapor feedback and global warming. Annu Rev Energy Environ 25(1):441–475
Hodnebrog Ø, Myhre G, Samset BH (2014) How shorter black carbon lifetime alters its climate effect. Nat Commun 5(1):1–7
Holland MM, Bitz CM (2003) Polar amplification of climate change in coupled models. Clim Dyn 21(3):221–232
Houghton JT, Ding YDJG, Griggs DJ, Noguer M, van der Linden PJ, Dai X et al (2001) Climate change 2001: the scientific basis. The Press Syndicate of the University of Cambridge, Cambridge
Huang Y, Xia Y, Tan X (2017) On the pattern of CO2 radiative forcing and poleward energy transport. J Geophys Res Atmos 122(20):10–578
Hunke EC, Lipscomb WH, Turner AK, Jeffery N, Elliott S (2010) Cice: the Los Alamos sea ice model documentation and software user's manual version 4.1 la-cc-06-012. T-3 Fluid Dyn Group Los Alamos Natl Lab 675:500
Joughin I, Alley RB, Holland DM (2012) Ice-sheet response to oceanic forcing. Science 338(6111):1172–1176
Karoly DJ (1990) The role of transient eddies in low-frequency zonal variations of the southern Hemisphere circulation. Tellus A Dyn Meteorol Oceanogr 42(1):41–50
Kay JE, Deser C, Phillips A, Mai A, Hannay C, Strand G, Arblaster JM, Bates SC, Danabasoglu G, Edwards J, Holland M, Kushner P, Lamarque J-F, Lawrence D, Lindsay K, Middleton A, Munoz E, Neale R, Oleson K, Polvani L, Vertenstein M (2015) The Community Earth System Model (CESM) large ensemble project: a community resource for studying climate change in the presence of internal climate variability. Bull Am Meteorol Soc 96(8):1333–1349
Lamarque JF, Shindell DT, Josse B, Young PJ, Cionni I, Eyring V, Faluvegi G, Folberth G, Ghan SJ, Horowitz LW, Lee YH, MacKenzie IA, Nagashima T, Naik V, Plummer D, Righi M, Rumbold ST, Schulz M, Skeie RB, Stevenson DS, Strode S, Sudo K, Szopa S, Voulgarakis A, Zeng G (2013) The Atmospheric Chemistry and Climate Model Intercomparison Project (ACCMIP): overview and description of models, simulations and climate diagnostics. Geosci Model Dev 6(1):179–206
Lawrence DM, Oleson KW, Flanner MG, Fletcher CG, Lawrence PJ, Levis S, Swenson SC, Bonan GB (2012) The CCSM4 land simulation, 1850–2005: assessment of surface climate and new capabilities. J Clim 25(7):2240–2260
Lenaerts JT, Fyke J, Medley B (2018) The signature of ozone depletion in recent Antarctic precipitation change: a study with the Community Earth System Model. Geophys Res Lett 45(23):12–931
Li X, Holland DM, Gerber EP, Yoo C (2014) Impacts of the north and tropical Atlantic Ocean on the Antarctic Peninsula and sea ice. Nature 505(7484):538–542
Li X, Cai W, Meehl GA, Chen D, Yuan X, Raphael M, Holland DM, Ding Q, Fogt RL, Markle BR, Wang G, Bromwich DH, Turner J, Xie S-P, Steig EJ, Gille ST, Xiao C, Wu B, Lazzara MA, Chen X, Stammerjohn S, Holland PR, Holland MM, Cheng X, Price SF, Wang Z, Bitz CM, Shi J, Gerber EP, Liang X, Goosse H, Yoo C, Ding M, Geng L, Xin M, Li C, Dou T, Liu C, Sun W, Wang X, Song C (2021) Tropical teleconnection impacts on Antarctic climate changes. Nat Rev Earth Environ 2(10):680–698
Liu F, Lu J, Garuba OA, Huang Y, Leung LR, Harrop BE, Luo Y (2018) Sensitivity of surface temperature to oceanic forcing via q-flux green's function experiments. Part II: feedback decomposition and polar amplification. J Clim 31(17):6745–6761
Liu F, Lu J, Huang Y, Leung LR, Harrop BE, Luo Y (2020) Sensitivity of surface temperature to oceanic forcing via q-flux Green's function experiments. Part III: asymmetric response to warming and cooling. J Clim 33(4):1283–1297
Lorenz DJ, Hartmann DL (2001) Eddy–zonal flow feedback in the southern Hemisphere. J Atmos Sci 58(21):3312–3327
Manabe S, Wetherald RT (1975) The effects of doubling the CO2 concentration on the climate of a general circulation model. J Atmos Sci 32(1):3–15
Marshall J, Armour KC, Scott JR, Kostov Y, Hausmann U, Ferreira D, Shepherd TG, Bitz CM (2014) The ocean's role in polar climate change: asymmetric Arctic and Antarctic responses to greenhouse gas and ozone forcing. Philos Trans R Soc A Math Phys Eng Sci 372(2019):20130040
Masson-Delmotte V, Kageyama M, Braconnot P, Charbit S, Krinner G, Ritz C, Guilyardi E, Jouzel J, Abe-Ouchi A, Crucifix M, Gladstone RM, Hewitt CD, Kitoh A, LeGrande AN, Marti O, Merkel U, Motoi T, Ohgaito R, Otto-Bliesner B, Peltier WR, Ross I, Valdes PJ, Vettoretti G, Weber SL, Wolk F, Yu Y (2006) Past and future polar amplification of climate change: climate model intercomparisons and ice-core constraints. Clim Dyn 26(5):513–529
Mayewski PA, Meredith MP, Summerhayes CP, Turner J, Worby A, Barrett PJ, Bracegirdle T, Naveira Garabato AC, Bromwich D, Campbell H, Hamilton GS, Lyons WB, Maasch KA, Aoki S, Xiao C, van Ommen T (2009) State of the Antarctic and southern Ocean climate system. Rev Geophys. https://doi.org/10.1029/2007RG000231
Monaghan AJ, Bromwich DH, Chapman W, Comiso JC (2008) Recent variability and trends of Antarctic near-surface temperature. J Geophys Res Atmos. https://doi.org/10.1029/2007JD009094
Myhre G, Shindell D, Pongratz J (2014) Anthropogenic and natural radiative forcing. In: Stocker T (ed) Climate change 2013: the physical science basis; Working Group I contribution to the fifth assessment report of the Intergovernmental Panel on Climate Change. Cambridge University Press, Cambridge
Oliva M, Navarro F, Hrbáček F, Hernandéz A, Nývlt D, Pereira P, Ruiz-Fernandéz J, Trigo R (2017) Recent regional climate cooling on the Antarctic Peninsula and associated impacts on the cryosphere. Sci Tot Environ 580:210–223
Payne AE, Jansen MF, Cronin TW (2015) Conceptual model analysis of the influence of temperature feedbacks on polar amplification. Geophys Res Lett 42(21):9561–9570
Pithan F, Mauritsen T (2014) Arctic amplification dominated by temperature feedbacks in contemporary climate models. Nat Geosci 7(3):181–184
Polvani LM, Waugh DW, Correa GJ, Son SW (2011) Stratospheric ozone depletion: the main driver of twentieth-century atmospheric circulation changes in the southern Hemisphere. J Clim 24(3):795–812
Polvani LM, Previdi M, England MR, Chiodo G, Smith KL (2020) Substantial twentieth-century Arctic warming caused by ozone-depleting substances. Nat Clim Change 10(2):130–133
Polvani LM, Banerjee A, Chemke R, Doddridge EW, Ferreira D, Gnanadesikan A, Holland MA, Kostov Y, Marshall J, Seviour WJM, Solomon S, Waugh DW (2021) Interannual SAM modulation of Antarctic Sea ice extent does not account for its long-term trends, pointing to a limited role for ozone depletion. Geophys Res Lett. https://doi.org/10.1029/2021GL094871
Previdi M, Polvani LM (2014) Climate system response to stratospheric ozone depletion and recovery. Q J R Meteorol Soc 140(685):2401–2419
Previdi M, Polvani LM (2017) Impact of the Montreal Protocol on Antarctic surface mass balance and implications for global sea level rise. J Clim 30(18):7247–7253
Pritchard H, Ligtenberg SR, Fricker HA, Vaughan DG, van den Broeke MR, Padman L (2012) Antarctic ice-sheet loss driven by basal melting of ice shelves. Nature 484(7395):502–505
Qian Y, Yasunari TJ, Doherty SJ, Flanner MG, Lau WK, Ming J, Wang H, Wang M, Warren SG, Zhang R (2015) Light-absorbing particles in snow and ice: measurement and modeling of climatic and hydrological impact. Adv Atmos Sci 32(1):64–91

Ramanathan V, Dickinson RE (1979) The role of stratospheric ozone in the zonal and seasonal radiative energy balance of the earth-troposphere system. J Atmos Sci 36(6):1084–1104
Ramanathan V, Callis L, Cess R, Hansen J, Isaksen I, Kuhn W, Lacis A, Luther F, Mahlman J, Reck R, Schlesinger M (1987) Climate–chemical interactions and effects of changing atmospheric trace gases. Rev Geophys 25(7):1441–1482
Ramaswamy V, Schwarzkopf MD, Shine KP (1992) Radiative forcing of climate from halocarbon-induced global stratospheric ozone loss. Nature 355(6363):810–812
Randel WJ, Wu F (1999) Cooling of the Arctic and Antarctic polar stratospheres due to ozone depletion. J Clim 12(5):1467–1479
Screen JA, Simmonds I (2010) The central role of diminishing sea ice in recent Arctic temperature amplification. Nature 464(7293):1334–1337
Serreze MC, Francis JA (2006) The Arctic amplification debate. Clim Change 76(3):241–264
Serreze MC, Barry RG (2011) Processes and impacts of Arctic amplification: a research synthesis. Glob Planet Change 77(1–2):85–96
Shell KM, Kiehl JT, Shields CA (2008) Using the radiative kernel technique to calculate climate feedbacks in NCAR's Community Atmospheric Model. J Clim 21(10):2269–2282
Shindell D, Faluvegi G, Nazarenko L, Bowman K, Lamarque JF, Voulgarakis A, Schmidt GA, Pechony O, Ruedy R (2013) Attribution of historical ozone forcing to anthropogenic emissions. Nat Clim Change 3(6):567–570
Shine KP (1991) On the cause of the relative greenhouse strength of gases such as the halocarbons. J Atmos Sci 48(12):1513–1518
Soden BJ, Held IM (2006) An assessment of climate feedbacks in coupled ocean–atmosphere models. J Clim 19(14):3354–3360
Soden BJ, Held IM, Colman R, Shell KM, Kiehl JT, Shields CA (2008) Quantifying climate feedbacks using radiative kernels. J Clim 21(14):3504–3520
Solomon S (1990) Progress towards a quantitative understanding of Antarctic ozone depletion. Nature 347(6291):347–354
Solomon S, Garcia RR, Rowland FS, Wuebbles DJ (1986) On the depletion of Antarctic ozone. Nature 321(6072):755–758
Song Y, Robinson WA (2004) Dynamical mechanisms for stratospheric influences on the troposphere. J Atmos Sci 61(14):1711–1725
Steig EJ, Schneider DP, Rutherford SD, Mann ME, Comiso JC, Shindell DT (2009) Warming of the Antarctic ice-sheet surface since the 1957 international geophysical year. Nature 457(7228):459–462
Stroeve JC, Serreze MC, Holland MM, Kay JE, Malanik J, Barrett AP (2012) The Arctic's rapidly shrinking sea ice cover: a research synthesis. Clim Change 110(3):1005–1027
Stuecker MF, Bitz CM, Armour KC, Proistosescu C, Kang SM, Xie SP, Kim D, McGregor S, Zhang W, Zhao S, Cai W, Dong Y, Jin FF (2018) Polar amplification dominated by local forcing and feedbacks. Nat Clim Change 8(12):1076–1081
Swart NC, Fyfe JC, Gillett N, Marshall GJ (2015) Comparing trends in the southern annular mode and surface westerly jet. J Clim 28(22):8840–8859
Tewari K, Mishra SK, Dewan A, Ozawa H (2021) Effects of the Antarctic elevation on the atmospheric circulation. Theor Appl Climatol 143(3):1487–1499
Thompson DW, Wallace JM, Hegerl GC (2000) Annular modes in the extratropical circulation. Part II: Trends. J Clim 13(5):1018–1036
Thompson DW, Furtado JC, Shepherd TG (2006) On the tropospheric response to anomalous stratospheric wave drag and radiative heating. J Atmos Sci 63(10):2616–2629
Thompson DW, Solomon S, Kushner PJ, England MH, Grise KM, Karoly DJ (2011) Signatures of the Antarctic ozone hole in southern Hemisphere surface climate change. Nat Geosci 4(11):741–749
Turner J, Colwell SR, Marshall GJ, Lachlan-Cope TA, Carleton AM, Jones PD, Lagun V, Reid PA, Iagovkina S (2005) Antarctic climate change during the last 50 years. Int J Climatol 25(3):279–294
Vaughan DG, Marshall GJ, Connolley WM, Parkinson C, Mulvaney R, Hodgson DA, King JC, Pudsey CJ, Turner J (2003) Recent rapid regional climate warming on the Antarctic Peninsula. Clim Change 60(3):243–274
Virgin JG, Smith KL (2019) Is Arctic amplification dominated by regional radiative forcing and feedbacks: perspectives from the world-avoided scenario. Geophys Res Lett 46(13):7708–7717
Wang Y, Huang G, Hu K (2020) Internal variability in multidecadal trends of surface air temperature over Antarctica in austral winter in model simulations. Clim Dyn 55(9):2835–2847
Wetherald RT, Manabe S (1988) Cloud feedback processes in a general circulation model. J Atmos Sci 45(8):1397–1416
Xia Y, Huang Y, Hu Y (2018) On the climate impacts of upper tropospheric and lower stratospheric ozone. J Geophys Res Atmos 123(2):730–739
Xia Y, Hu Y, Liu J, Huang Y, Xie F, Lin J (2020) Stratospheric ozone-induced cloud radiative effects on Antarctic sea ice. Adv Atmos Sci 37:505–514
Zelinka MD, Klein SA, Hartmann DL (2012) Computing and partitioning cloud feedbacks using cloud property histograms. Part I: cloud radiative kernels. J Clim 25(11):3715–3735
Zhang R, Wang H, Fu Q, Pendergrass AG, Wang M, Yang Y, Ma PL, Rasch PJ (2018) Local radiative feedbacks over the Arctic based on observed short-term climate variations. Geophys Res Lett 45(11):5761–5770

Publisher's Note

Springer Nature remains neutral with regard to jurisdictional claims in published maps and institutional affiliations.